

# $\mu$ -Phone: Accessible Microscope Attachment for Smartphones

Kefan Song<sup>1</sup>, Sixuan Wu<sup>2</sup>, Ruijia Peng<sup>3</sup>, Jason Cobb<sup>4</sup>, and Alexander T Adams<sup>2</sup>

<sup>1</sup>Wallace H. Coulter Department of Biomedical Engineering, Georgia Institute of Technology, Atlanta, GA, USA

<sup>2</sup>School of Interactive Computing, Georgia Institute of Technology, Atlanta, GA, USA

<sup>3</sup>School of Computer Science, Georgia Institute of Technology, Atlanta, GA, USA

<sup>4</sup>Renal Medicine, Emory University School of Medicine, Atlanta, GA, USA

{ksong75, swu469, rpeng37, aadams322}@gatech.edu  
jcobb2@emory.edu

**Abstract**—Point-of-care (POC) technologies have the potential to greatly improve the clinical lab testing and diagnostics process since they significantly reduce the wait time before getting the results. Microscope, as a very important instrument widely used in clinical testing, is a key component to be adapted to POC scenarios, and there have been various attempts to do so by replacing conventional microscopes with smartphone-attached systems. However, these attempts all utilized components that are either expensive or bulky, which greatly limits the widespread adaptation and utilization of these devices, especially in areas with limited resources. Thus we propose a design and prototype of  $\mu$ -Phone, an accessible microscope attachment for smartphones using cheap and easily accessible components to minimize the obstacles to resource availability. The proposed system has a depth of field of 5.25 micrometers, a pixel resolution of 26.3 pixels per micrometer and a spatial resolution of 2.19 micrometers, which makes it powerful enough to capture microscopic images for identification and analysis at a cellular level. With some future developments, this system has great potential to be deployed worldwide for quick and accurate POC analysis of physiological samples.

**Index Terms**—point-of-care, microscope, accessibility, healthcare, smartphone

## I. INTRODUCTION

The compound microscope is an indispensable tool for clinical pathology and laboratory medicine, both of which are crucial components of accurate and timely diagnosis in healthcare [1]. However, such services are very limited and often inaccessible to most patients in low-income and middle-income countries [2]. As a result, point-of-care (POC) imaging technologies serve as an important alternative due to their ease of use, ability to deliver rapid diagnoses, and elimination of the need for extensive laboratory facilities [3]. In this context, the widespread adoption of smartphones globally, combined with their robust data processing capabilities and high-performance sensors, makes them an ideal platform for integrating POC imaging technologies [4].

Previous work on integrating microscopy with mobile phones has demonstrated promising results but often falls short in terms of accessibility and practicality for widespread use. As one of the early attempts, Skandarajah et al. developed a mobile phone microscope with lens components from commercial microscopes [5], which are very expensive. This

prototype is also designed as a desktop device due to its bulky nature. Switz et al. utilized a camera lens system from a dismantled smartphone camera in reverse to achieve microscopic magnification [6], but the availability of dismantled camera lens systems is limited and not easily accessible to the general public. Its bulky design also restricts its use to desktop settings. Similarly, the microscope design by Pirstill and Coté [7], although handheld, was not compact or cheap enough due to the use of an objective lens from commercial microscopes. Agbana et al. [8] proposed using a single ball lens for microscopic imaging, which effectively limits the form factor of the optical system. However, their image quality deteriorates drastically at off-center locations due to the high aberration and vignetting effects of the ball lens. Additionally, all these works utilized external light sources, contributing to both system complexity and extra cost. These limitations underscore the need for a more compact and accessible mobile phone microscope solution that can be easily deployed and operated in low-resource settings.

In this work,  $\mu$ -Phone, an accessible microscope attachment for smartphones, is proposed. This attachment utilizes an optical system that does not require professional optical-grade components and operates without external power or lighting sources. It is compact and lightweight, designed as a phone case that can easily fit into most clothes pockets. The  $\mu$ -Phone achieves high magnification using cheap lenses and the smartphone's built-in camera application, with a depth

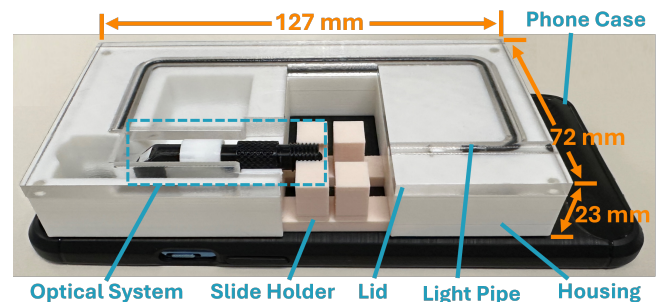


Fig. 1. Prototype of the  $\mu$ -Phone with a clear lid to show major components of the system.

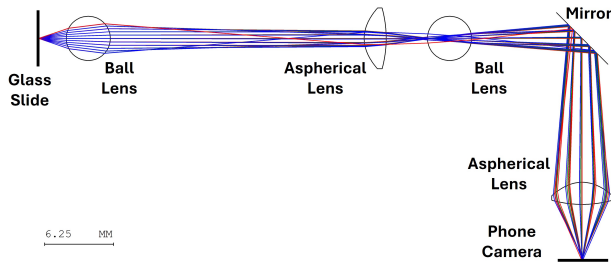


Fig. 2. Ray diagram of the magnifying optical system consists of two ball lenses, two aspherical lenses, and a mirror.

of field of  $5.25 \mu\text{m}$ , a pixel resolution of  $26.3 \text{ px}/\mu\text{m}$  and a spatial resolution of over  $2.19 \mu\text{m}$ . All components can be easily purchased from major online vendors for a total cost of less than \$20. The capabilities of the  $\mu$ -Phone system are demonstrated using optical target slides, and its application in healthcare is shown through the observation of common biological samples.

## II. MATERIALS AND METHODS

The system design is illustrated in Fig. 1. It consists of an optical system, a moving slide holder, a light pipe, and hardware housing, and is glued onto a commodity phone case. Most optical devices nowadays use custom-made lenses specifically for optical applications, which are expensive and not easy to acquire. To make our system more accessible, the lens components are chosen to be aspherical lenses originally used in laser pointers for light collimation as well as quartz beads originally used for ball vaping. Both these lenses can be obtained very easily since they are both very cheap and are manufactured in large quantities.

### A. Optical System Design

The lenses of choice are 4mm diameter quartz ball lenses (Amazon, Beracky 4mm Clear Quartz Balls Beads Insert) and 5mm outer diameter acrylic aspherical lenses (Amazon, Qiaoba Laser Lens Focus 4mm Aspherical Lens 5mm Diameter Collimating Lens for Laser Module). The equations describing the specific surface of the aspherical lens are derived by fitting equations to the edges of its cross-sectional profiles. Ball lenses were chosen due to their high magnification ratio, but since they also introduce a large amount of aberrations, the image was corrected with the aspherical lens right afterward. This combination was then replicated to achieve the desired magnification level. The distances between each lens were estimated and measured on an optical rail system and fine-tuned in optical design software (CODE V, Synopsys, Sunnyvale, CA). The ray diagram of the entire optical system is shown in Fig. 2. A square mirror tile with a 5mm side length (Amazon, Self-Adhesive Real Glass Craft Mini Square Round Mirrors Mosaic Tiles 5 x 5mm) was put between the second ball lens and the aspherical lens at a  $45^\circ$  angle so the majority of the optical system lays parallel to the phone to make the system more compact.

### B. Microscope Housing Design and Fabrication

The housing design and setup for the microscope are shown in Fig. 1. The total dimension of the housing is  $127\text{mm} \times 72\text{mm} \times 23\text{mm}$ , which is compact enough to fit in most clothes pockets. Lens barrels were designed and 3D-printed according to the optical system parameters and the lenses were press-fitted into corresponding locations. A light pipe (LC2-10.0, Bivar Inc.) that was reshaped under heat was used to direct the light from the phone flashlight as the backlight of the microscope. A threaded connection between the optical system and the glass slide holder enables focus plane fine-tuning capability. The housing was 3D printed using Bambu Lab X1-Carbon 3D printer (Bambulab USA Inc., Austin, TX) and glued to a commodity smartphone case. A lid was also 3D-printed to fix all components properly.

### C. Image Acquisition and Analysis

The smartphone used in this study is the OnePlus 9 from OnePlus Technologies Co., Ltd., which is equipped with Sony IMX689 image sensor (48 megapixels,  $1.12\mu\text{m}$  per pixel, 23mm equivalent focal length, 1.8  $f$ -number) for its primary camera. All automatic settings, including high dynamic range and filters, were disabled to avoid software-based photo enhancements. The high-resolution mode of the built-in camera application was used for all image acquisition tasks to fully utilize the sensor's 48 megapixel capacity. Raw images were processed using OpenCV (<https://opencv.org>) in Python, and all analyses were performed in Matlab (R2024a, MathWorks, Natick, MA).

### D. Sample preparation

The image quality of the  $\mu$ -Phone was evaluated using a grid distortion target and a resolution target. The grid distortion target was purchased from Thorlabs with grid spacing down to 10 micrometers (R1L3S3P, Thorlabs Inc., Newton, NJ). The resolution target was also purchased from Thorlabs with 1951 USAF targets from group +2 to group +7 (R3L1S4P, Thorlabs Inc., Newton, NJ).

In addition, a blood smear was prepared for observation of human red blood cells under the  $\mu$ -Phone. With informed consent, a drop of finger-pricked blood was collected from one of the authors, spread across a glass slide, and allowed to dry before microscopic examination.

## III. RESULTS

The processing pipeline for images taken with the  $\mu$ -Phone is shown in Fig. 3. Raw images are preprocessed by cropping to remove extraneous regions before being converted to greyscale for uniform analysis. A circular boundary mask is then applied to isolate the field-of-view (FOV) region. Following preprocessing, the images undergo a series of processing steps. First, min-max normalization is used to scale the pixel intensity values, enhancing the dynamic range. Gaussian filtering is applied to reduce high-frequency noise while preserving edges, and sharpening is performed afterward to enhance the edge and fine details of the image. Median filtering further

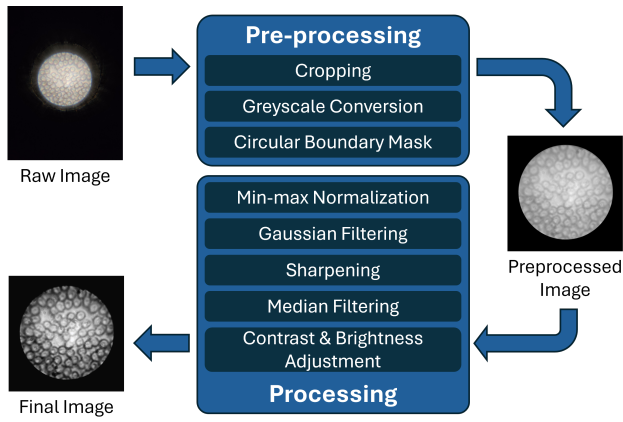


Fig. 3. Processing flowchart for images taken with  $\mu$ -Phone.

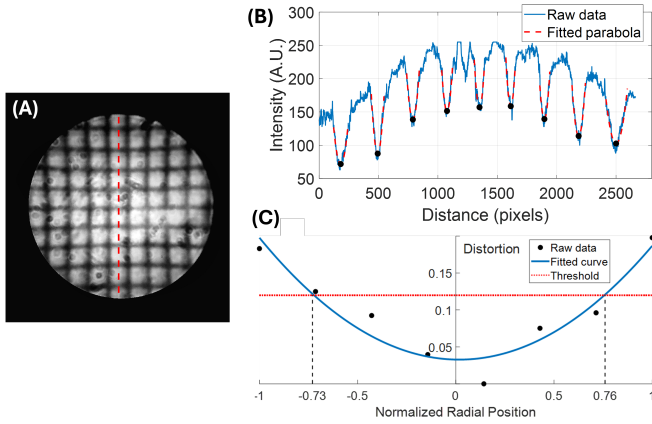


Fig. 4. (A) Processed image of a  $10\ \mu\text{m}$  spacing grid distortion target acquired using  $\mu$ -Phone. (B) Intensity profile of pixels marked with the dotted line in (A); Dashed parabolas are the best-fitted quadratic functions for each convex section and black dots are the vertices of the corresponding parabola. (C) Spatial distortion across the FOV with a parabolic fit as well as the distortion threshold for commercial microscope eyepieces.

reduces noise, particularly speckle noise, and finally contrast and brightness adjustments are made to optimize the visibility of the structures within the image. These sequential processing steps ensure optimal contrast and edge sharpness, providing high-quality images for further analysis.

#### A. Optical Design Characterization

The depth of field of the  $\mu$ -Phone,  $D_f$ , was calculated from:

$$D_f = \frac{n\lambda}{NA^2},$$

where  $n$  is the refractive index of the medium between the objective lens and the object,  $\lambda$  is the wavelength of the light source, and  $NA$  is the numerical aperture of the objective lens [9]. Since the system operates in air with a white light source, we assumed  $n = 1$  and used average wavelength  $\lambda = 0.54\ \mu\text{m}$ . The numerical aperture ( $NA$ ) of the objective lens was measured to be 0.32, resulting in a calculated depth of field  $D_f = 5.25\ \mu\text{m}$ .

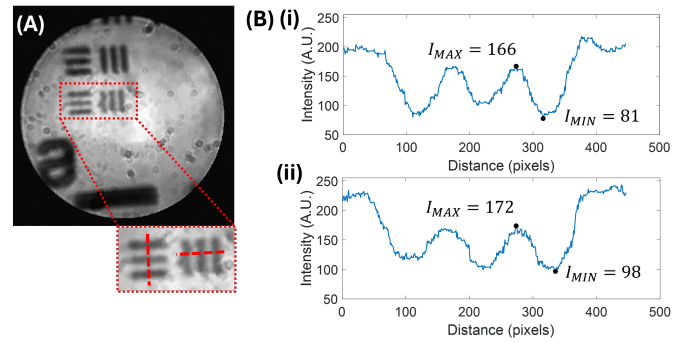


Fig. 5. (A) Processed image of the 1951 USAF resolution target acquired using  $\mu$ -Phone showing elements 5 and 6 of Group +7. (B) Intensity profile of the pixels across the (i) horizontal and (ii) vertical line bars as shown with dotted lines in (A).

Image properties of the  $\mu$ -Phone, such as pixel resolution, FOV, and distortion were estimated through imaging a  $10\ \mu\text{m}$  spacing grid distortion target as shown in Fig. 4(A). Based on the number of visible gridlines, the FOV of the system was determined to be approximately  $90\ \mu\text{m}$  in diameter. A column of pixels at the center of the image was selected, and its pixel intensities were plotted and processed, as shown in Fig. 4(B). In this plot, each convex area represents the cross-section of a gridline. Parabolas were fitted to each convex section and the vertices of those parabolas were treated as the centers of the gridlines. The pixel resolution was calculated from the radial spacing between the two adjacent gridlines at the center of the image and was found to be  $26.3\ \text{px}/\mu\text{m}$ . Image distortion was calculated as the percentage increase in adjacent gridline spacing relative to the center and was plotted in Fig. 4(C). Typical professional-grade microscope eyepieces maintain a maximum distortion of less than 12% across the entire field of view [5], and the  $\mu$ -Phone achieves this same level of distortion within the central 75% radius of its images, while the maximum distortion at the outer regions remains under 20%, which is considered acceptable for a low-cost, portable solution.

The spatial resolution of the  $\mu$ -Phone was demonstrated by imaging a 1951 USAF resolution target. The pixel intensities across the horizontal and vertical line pairs of group +7, element 6, were plotted, as shown in Fig. 5. The Michelson contrast ( $C = \frac{I_{MAX} - I_{MIN}}{I_{MAX} + I_{MIN}}$ ) was calculated to be 34% and 27%, respectively, indicating good image contrast for this group. Since it is the smallest element available on the resolution target, the resolution of the system was determined to be smaller than  $2.19\ \mu\text{m}$ .

#### B. Blood Observation Application

To evaluate the ability of the  $\mu$ -Phone to observe biological specimens, especially blood samples, pictures of the prepared blood smear were taken with both the  $\mu$ -Phone and a traditional laboratory microscope (Fisherbrand™ Research Grade Upright Microscope, Thermo Fisher Scientific, Waltham, MA), as shown in Fig. 6. This figure shows that although the image



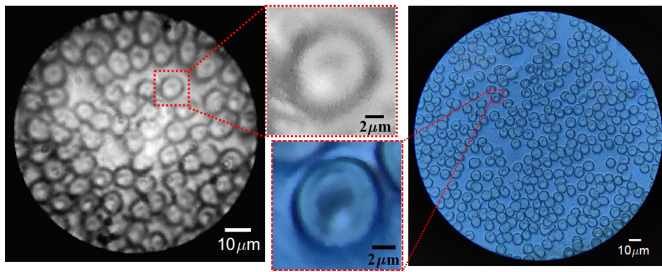


Fig. 6. (A) Processed image of a human blood smear acquired using  $\mu$ -Phone with an enlarged view of a red blood cell. (B) Cropped image of the same blood smear acquired using a traditional laboratory microscope.

contrast of the  $\mu$ -Phone is not as good as the commercial product, it has a greater magnification ratio and is still capable of capturing the morphological features of the red blood cell.

### C. Cost of Production

The optical system of the  $\mu$ -Phone utilizes two aspherical lenses and quartz beads each, as well as a mirror tile, which costs \$3.5 in total. The light pipe costs \$3.96 individually and could be less than \$2 when purchased in bulk. The generic phone case could be purchased for around \$10, and all 3D-printed parts used about 80g of PLA material, which corresponds to about \$1.6 for the cost of filaments. Thus, the overall material cost for the entire system is less than \$20, which is substantially cheaper than any existing product with comparable magnification power.

### IV. DISCUSSION

The above experimental findings indicate that the  $\mu$ -Phone system is capable of generating images at a microscopic level that is sufficient for the identification and analysis of individual human blood cell samples. Additionally, ray-tracing simulation indicate that dimensional errors in the 3D-printed lens barrel, such as a 0.5 mm change in the distance between lenses, would only result in a 0.1 mm shift of the image plane, which can be easily corrected by fine-tuning the object focus. This ensures that image quality of the system remains unaffected with most commonly used 3D printers, which can easily achieve precision better than 0.5 mm. Combined with its low material cost and the ease of acquiring all needed materials from online vendors, the  $\mu$ -Phone system is highly accessible, especially in regions with limited access to clinical laboratories.

As the  $\mu$ -Phone was developed as a proof-of-concept prototype, it could be further improved in terms of its functions and performances. On the software side, alternative camera applications may be able to improve image quality by adjusting properties like contrast and sharpness of the raw image sensor data as well as calibrating for distortions. Additional features like cell recognition and counting could also be developed. On the hardware side, brighter and more uniform illumination of the FOV area could be achieved with an improved light transmission mechanism from the flashlight. Support for microfluidic tubes and channels could also be incorporated for easier preparation of biological fluid samples.

These future developments and improvements amplify the potential of the widespread deployment of the  $\mu$ -Phone as a powerful, accessible, and portable device for POC testing.

### V. CONCLUSION

In this work, we present the  $\mu$ -Phone, a smartphone-attached microscope system that is cheap and accessible. Through observing optical target slides and blood smear samples, we demonstrated this system's capability to capture micrometer-level objects, namely red blood cells, for clinical analysis at a cellular level. The significantly lowered cost of the system, the extremely compact form factor, as well as the ease of its production process all make POC blood tests a lot more accessible and scalable. This system fully utilizes the power of smartphones for POC testing technologies, and it serves as a fundamental prototype for integrating various more specific lab test capabilities in the future.

### REFERENCES

- [1] Jesus Salido et al. "A review on low-cost microscopes for Open Science". In: *Microscopy Research and Technique* 85.10 (Oct. 2022), pp. 3270–3283. ISSN: 10970029. DOI: 10.1002/jemt.24200.
- [2] Michael L Wilson et al. "Access to pathology and laboratory medicine services: a crucial gap". en. In: *The Lancet* 391.10133 (May 2018), pp. 1927–1938. ISSN: 01406736. DOI: 10.1016/S0140-6736(18)30458-6.
- [3] Michel Drancourt et al. "The Point-of-Care Laboratory in Clinical Microbiology". en. In: *Clinical Microbiology Reviews* 29.3 (July 2016), pp. 429–447. ISSN: 0893-8512, 1098-6618. DOI: 10.1128/CMR.00090-15.
- [4] Junjie Liu et al. "Point-of-care testing based on smartphone: The current state-of-the-art (2017–2018)". en. In: *Biosensors and Bioelectronics* 132 (May 2019), pp. 17–37. ISSN: 09565663. DOI: 10.1016/j.bios.2019.01.068.
- [5] Arunan Skandarajah et al. "Quantitative Imaging with a Mobile Phone Microscope". en. In: *PLOS ONE* 9.5 (May 2014), e96906. ISSN: 1932-6203. DOI: 10.1371/journal.pone.0096906.
- [6] Neil A. Switz, Michael V. D'Ambrosio, and Daniel A. Fletcher. "Low-Cost Mobile Phone Microscopy with a Reversed Mobile Phone Camera Lens". en. In: *PLOS ONE* 9.5 (May 2014). Ed. by Madhukar Pai, e95330. ISSN: 1932-6203. DOI: 10.1371/journal.pone.0095330.
- [7] Casey W. Pirnstill and Gerard L. Coté. "Malaria Diagnosis Using a Mobile Phone Polarized Microscope". en. In: *Scientific Reports* 5.1 (Aug. 2015), p. 13368. ISSN: 2045-2322. DOI: 10.1038/srep13368.
- [8] Temitope E. Agbana et al. "Imaging & identification of malaria parasites using cellphone microscope with a ball lens". en. In: *PLOS ONE* 13.10 (Oct. 2018). Ed. by Kristen C. Maitland, e0205020. ISSN: 1932-6203. DOI: 10.1371/journal.pone.0205020.
- [9] Douglas B. Murphy. *Fundamentals of light microscopy and electronic imaging*. en. New York: Wiley-Liss, 2001. ISBN: 978-0-471-25391-4.